Benchmarking of B2 Code with a One-Dimensional Plasma Fluid Model Incorporating Anisotropic Ion Pressures on Simple Mirror Configurations*)

Satoshi TOGO, Dirk REISER[1)], Petra BÖRNER[1)], Mizuki SAKAMOTO, Naomichi EZUMI and Yousuke NAKASHIMA

Plasma Research Center, University of Tsukuba, Tsukuba 305-8577, Japan
[1)]*Forschungszentrum Jülich GmbH, IEK-Plasmaphysik, Jülich 52425, Germany*

(Received 28 December 2017 / Accepted 25 February 2018)

A plasma fluid code B2 has been benchmarked with a one-dimensional plasma fluid model incorporating the anisotropic ion pressures (AIP model) on simple mirror configurations. In a low collisionality case, profiles of plasma parameters of the B2 code deviate from those of the AIP model. The validity of the viscous-flux approximation is investigated by direct comparisons with the anisotropic part of the ion pressure indicating the invalidity of the viscous-flux approximation is considered to be responsible to deviations of profiles. In addition, supersonic plasma flows downstream from the mirror throat are observed.

Keywords: plasma fluid model, B2 code, anisotropic ion pressures, viscous-flux approximation, diverging magnetic field, supersonic plasma flow

DOI: 10.1585/pfr.13.3403022

1. Introduction

In order to design a divertor in a future fusion reactor such as DEMO or estimate an operation window for detached plasmas, it is crucial to develop a robust model to predict profiles of scrape-off layer (SOL)-divertor plasma parameters. Various SOL-divertor plasma code packages, therefore, have been developed and benchmarked with experimental results such as SOLPS (B2-EIRENE) [1], SONIC [2, 3] and UEDGE [4]. Experimental results of existing devices, however, cannot always be reproduced satisfactorily with these code packages and efforts have been made to resolve this issue from, for example, kinetic effects of a plasma [5], drifts [6, 7], supersonic plasma flows [8], neutral models [5, 6], impurity models [9] and plasma-wall-interactions (PWI) models [7, 8] points of view.

In a SOL-divertor region of a typical torus device with an aspect ratio of $R/a \sim 3$, the spatial variation of the magnetic field strength B becomes a factor of ~ 2. In such a condition, contribution of the mirror force can be comparable to the pressure-gradient force and largely alter the flow velocity profile [10]. In addition, it is expected that supersonic plasma flows occur in diverging magnetic fields. In the Braginskii's plasma fluid model [11] which is used in code packages mentioned above, however, a viscous-flux approximation is included in the mirror force term and the pressure-gradient force term. Therefore, it is an important issue to investigate the validity of this viscous-flux approximation in inhomogeneous magnetic field configurations.

We have been developing a one-dimensional plasma fluid model incorporating the anisotropic ion pressures (AIP model) [12, 13]. The viscous-flux used in the Braginskii's plasma fluid model is an approximation of the anisotropic part of the ion pressure. Thus, by directly incorporating the anisotropic ion pressures into a plasma fluid model, a viscous-flux approximation becomes no longer necessary and the above-mentioned force terms become free of any approximations. Therefore, the validity of the viscous-flux approximation can be studied by direct comparisons between the Braginskii's plasma fluid model and the AIP model.

In order to obtain comprehensible results and useful insights, we use simple mirror configurations instead of real SOL-divertor configurations in this paper. As one of SOL-divertor plasma codes based on the Braginskii's plasma fluid model, we use a two-dimensional code B2 [14] which has been applied not only to SOL-divertor plasmas in tokamaks but also to plasmas in linear devices [15]. In Sec. 2, the AIP model, the B2 code and calculation conditions are briefly explained. Results are shown in Sec. 3. Section 4 summarizes this paper.

2. Numerical Models

2.1 Anisotropic-ion-pressure (AIP) model

Basic equations for a plasma in the AIP model are written as follows [12, 13];

$$\frac{\partial n}{\partial t} + B\frac{\partial}{\partial s}\left(\frac{nV}{B}\right) = S, \tag{1}$$

author's e-mail: togo@prc.tsukuba.ac.jp

*) This article is based on the presentation at the 26th International Toki Conference (ITC26).

$$\frac{\partial}{\partial t}\left(m_{\rm i}nV\right)+B\frac{\partial}{\partial s}\left[\frac{1}{B}\left(m_{\rm i}nV^2+p_{\rm i,\parallel}+p_{\rm e}\right)\right]+\frac{p_{\rm i,\perp}+p_{\rm e}}{B}\frac{\partial B}{\partial s}=M_{\rm m}, \tag{2}$$

$$\frac{\partial}{\partial t}\left(\frac{1}{2}m_{\rm i}nV^2+\frac{1}{2}p_{\rm i,\parallel}\right)+B\frac{\partial}{\partial s}\left[\frac{1}{B}\left(\frac{1}{2}m_{\rm i}nV^3+\frac{3}{2}p_{\rm i,\parallel}V+q_{\rm i,\parallel}\right)\right]+\frac{p_{\rm i,\perp}V+q_{\rm i,\perp}}{B}\frac{\partial B}{\partial s}=Q_{\rm i,\parallel}+\frac{p_{\rm i,\perp}-p_{\rm i,\parallel}}{\tau_{\rm rlx}}+\frac{m_{\rm e}}{m_{\rm i}}\frac{p_{\rm e}-p_{\rm i,\parallel}}{\tau_{\rm e}}-V\frac{\partial p_{\rm e}}{\partial s}, \tag{3}$$

$$\frac{\partial p_{\rm i,\perp}}{\partial t}+B\frac{\partial}{\partial s}\left(\frac{p_{\rm i,\perp}V+q_{\rm i,\perp}}{B}\right)-\frac{p_{\rm i,\perp}V+q_{\rm i,\perp}}{B}\frac{\partial B}{\partial s}=Q_{\rm i,\perp}+\frac{p_{\rm i,\parallel}-p_{\rm i,\perp}}{\tau_{\rm rlx}}+\frac{2m_{\rm e}}{m_{\rm i}}\frac{p_{\rm e}-p_{\rm i,\perp}}{\tau_{\rm e}}, \tag{4}$$

$$\frac{\partial}{\partial t}\left(\frac{3}{2}p_{\rm e}\right)+B\frac{\partial}{\partial s}\left[\frac{1}{B}\left(\frac{5}{2}p_{\rm e}V+q_{\rm e}\right)\right]=Q_{\rm e}+\frac{3m_{\rm e}}{m_{\rm i}}\frac{p_{\rm i}-p_{\rm e}}{\tau_{\rm e}}+V\frac{\partial p_{\rm e}}{\partial s}. \tag{5}$$

Equations (1) - (5) are of continuity of ion, parallel momentum of plasma, parallel component of ion energy, perpendicular component of ion energy and electron energy, respectively. Here, the pressure is defined by $p_\sigma = nT_\sigma$ in which σ represents the species and components as $\sigma \in \{(\mathrm{i},\parallel),(\mathrm{i},\perp),\mathrm{i},\mathrm{e}\}$. Other notations are the same as Ref. [16]. The ion-pressure relaxation time is given by $\tau_{\rm rlx} = 2.5\tau_{\rm i}$ [17] where the ion-ion Coulomb collision time $\tau_{\rm i}$ is estimated by using the effective-isotropic ion temperature $T_{\rm i} \equiv \left(T_{\rm i,\parallel}+2T_{\rm i,\perp}\right)/3$. The electron conductive heat flux $q_{\rm e}$ is estimated by a harmonic average of the Spitzer-Härm heat conduction $q_{\rm e}^{\rm SH} = -\kappa_{\rm e}^{\rm SH}\left(\partial T_{\rm e}/\partial s\right)$ and a free-streaming heat flux $q_{\rm e}^{\rm FS} = nT_{\rm e}\sqrt{T_{\rm e}/m_{\rm e}}$ as $q_{\rm e} = \left[1/q_{\rm e}^{\rm SH}+1/\left(\alpha_{\rm e}q_{\rm e}^{\rm FS}\right)\right]^{-1}$ in which the heat-flux limiting factor of electron is set to be $\alpha_{\rm e} = 0.5$. The ion conductive heat fluxes, $q_{\rm i,\parallel}$ and $q_{\rm i,\perp}$, are estimated by Spitzer-Härm heat conductions with the same settings as Refs. [18, 19]. The virtual divertor model [19] is used for the Bohm criterion at the sheath entrance.

2.2 B2 code

Although the B2 is a two-dimensional code, we apply it to a one-dimensional system by neglecting all of radial transports for simplicity in order to focus only on the parallel transport. By rewriting Eq. (2) in terms of $p_{\rm i} \equiv \left(p_{\rm i,\parallel}+2p_{\rm i,\perp}\right)/3$ and $\delta p_{\rm i} \equiv 2\left(p_{\rm i,\parallel}-p_{\rm i,\perp}\right)/3$ instead of $p_{\rm i,\parallel}$ and $p_{\rm i,\perp}$, we obtain the equivalent equation of parallel momentum of plasma in the Braginskii's plasma fluid model as follows;

$$\frac{\partial}{\partial t}\left(m_{\rm i}nV\right)+B\frac{\partial}{\partial s}\left(\frac{m_{\rm i}nV^2}{B}\right)+B^{3/2}\frac{\partial}{\partial s}\left(B^{-3/2}\delta p_{\rm i}\right)=-\frac{\partial}{\partial s}\left(p_{\rm i}+p_{\rm e}\right)+M_{\rm m}. \tag{6}$$

In addition, following viscous-flux approximation is applied;

$$\delta p_{\rm i} \approx -\eta_{\rm i}B^{-1/2}\frac{\partial}{\partial s}\left(B^{1/2}V\right) \equiv \pi_{\rm i}. \tag{7}$$

Here, the parallel-ion viscosity $\eta_{\rm i}$ is estimated in the B2 code as follows;

$$\left(1+\Omega_\eta\right)\eta_{\rm i} = \eta_{\rm cl} \equiv 0.96p_{\rm i}\tau_{\rm i},\ \Omega_\eta = \frac{\eta_{\rm cl}}{\beta p_{\rm i}}\left|\frac{\partial V}{\partial s}\right|. \tag{8}$$

In this study, we use a viscous-flux limiting factor $\beta = 0.5$. For the Bohm criterion, $V \geq c_{\rm s}$ is imposed in which $c_{\rm s} \equiv \sqrt{\left(T_{\rm i}+T_{\rm e}\right)/m_{\rm i}}$ is the plasma sound speed.

By summing Eqs. (3) and (4), we obtain the equivalent equation of ion energy in the Braginskii's plasma fluid model as follows;

$$\frac{\partial}{\partial t}\left(\frac{1}{2}m_{\rm i}nV^2+\frac{3}{2}p_{\rm i}\right)+B\frac{\partial}{\partial s}\left[\frac{1}{B}\left(\frac{1}{2}m_{\rm i}nV^3+\frac{5}{2}p_{\rm i}V+\pi_{\rm i}V+q_{\rm i}\right)\right]=Q_{\rm i}+\frac{3m_{\rm e}}{m_{\rm i}}\frac{p_{\rm e}-p_{\rm i}}{\tau_{\rm e}}-V\frac{\partial p_{\rm e}}{\partial s}. \tag{9}$$

Here, the ion conductive heat flux $q_{\rm i}$ is estimated by the Spitzer-Härm heat conduction $q_{\rm i}^{\rm SH} = -\kappa_{\rm i}^{\rm SH}\left(\partial T_{\rm i}/\partial s\right)$.

2.3 Calculation conditions

We have tried various kinds of simple mirror configurations in this benchmark study. In this paper, however, we only focus on one of them due to limitations of space. Comprehensive results including other configurations will be reported near future. Figure 1 (a) shows the parallel-to-$\boldsymbol{B}$ profile of the magnetic field strength B used in this paper in which the mirror ratio is $B_{\rm max}/B_{\rm min} \sim 4$. The system length is $L = 2.8$ m. The cross-sectional area of the flux tube A is also given as shown here satisfying the conservation of magnetic flux $\Phi = BA$. The particle source term is artificially given by $S = S_0\exp\left[-20\left(s/L\right)^2\right]$

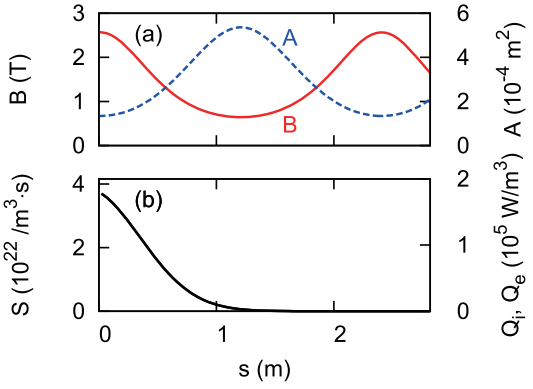

Fig. 1 Calculation conditions used in this paper; parallel-to-$\boldsymbol{B}$ profiles of (a) B (solid line), A (broken line) and (b) source terms in the case of $S_0 = 3.70\times10^{22}$ /m^3· s and $T_{\rm in} = 20$ eV.

as shown in Fig. 1 (b). Heat source terms are given by $Q_i = Q_e = (3/2)\,T_{in}S$ in which T_{in} is the source temperature. The ion heat source Q_i is divided into $Q_{i,\parallel} = Q_i/3$ and $Q_{i,\perp} = 2Q_i/3$ assuming isotropic heat sources for the AIP model. The absolute values of S_0 and T_{in} are changed as $S_0 = (1.85, 3.70, 7.40) \times 10^{22}$ /m^3·s and $T_{in} = 10, 20, 40$ eV in order to change the plasma collisionality resulting in nine cases of different plasma collisionalities totally. The momentum source M_m is set to be zero. A mirror symmetry condition is imposed at $s = 0$ as $\partial n/\partial s = \partial T/\partial s = V = 0$ and we set a sheath entrance at $s = L$. Deuterium ions are assumed in this study.

3. Results

The ion temperature anisotropy $T_{i,\parallel}/T_{i,\perp}$ estimated at $s = L$ by the AIP model is shown in Fig. 2 as a function of the ion collisionality L/λ_{mfp}. The mean free path of ion-ion Coulomb collisions λ_{mfp} is estimated by $\lambda_{mfp} = \tau_i \sqrt{T_{i,\parallel}/m_i}$. The ion temperature tends to be anisotropic in collisionless conditions even if the ion heat sources $Q_{i,\parallel}$ and $Q_{i,\perp}$ are given isotropically because the parallel component of energy is much easier to be lost than the perpendicular one by the convection. As the ion collisionality becomes higher, the ion temperature becomes more isotropic due to the collisional relaxation.

Figure 3 shows the profiles of plasma parameters for the highest collisionality case in Fig. 2 (i.e. $L/\lambda_{mfp} \approx 30$) generated with $S_0 = 7.40 \times 10^{22}$ /m^3· s and $T_{in} = 10$ eV. Note that in this figure and the following Fig. 4, the Mach profiles of the AIP model are estimated by the flow velocity normalized by the plasma sound speed using the parallel ion temperature $T_{i,\parallel}$, i.e. $c_s \equiv \sqrt{(T_{i,\parallel} + T_e)/m_i}$. In this high collisionality case, the profiles of the B2 code agree well with those of the AIP model except for the vicinity of the sheath entrance $s = L$. This deviation probably comes from the treatment of the Bohm criterion in the B2 code in which a linear extrapolation of V is applied when it tends to be higher than c_s. The sonic point is at the mirror throat ($s = 2.5$ m) and we have supersonic plasma flows downstream from there.

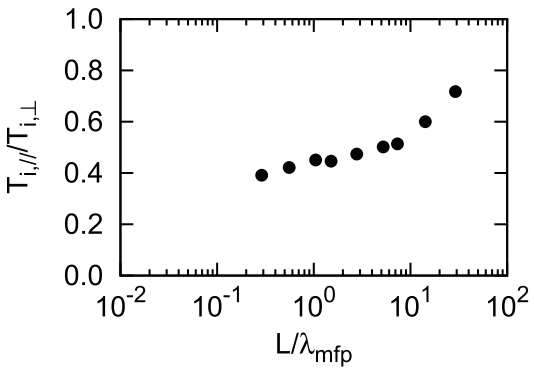

Fig. 2 T_i anisotropy, $T_{i,\parallel}/T_{i,\perp}$, estimated at $s = L$ by the AIP model as a function of the ion collisionality L/λ_{mfp}.

In Fig. 4, the profiles of plasma parameters for the lowest collisionality case in Fig. 2 (i.e. $L/\lambda_{mfp} \approx 0.3$) generated with $S_0 = 1.85 \times 10^{22}$ /m^3· s and $T_{in} = 40$ eV are shown. In this case, we can see deviations at the vicinity of the sheath entrance again which is the same tendency as the highest collisionality case. Except for this region, the temperature profiles of the B2 code are qualitatively similar to those of the AIP model in that they tend to be flat due to high conductivities. The profiles of the plasma density n and the Mach number M of the B2 code, however, deviate by a factor of ~ 2 from those of the AIP model in the region of a diverging magnetic field ($s = 0 \sim 1.25$ m).

Figure 5 shows direct comparisons of profiles of the viscous flux π_i and the anisotropic part of the ion pressure δp_i estimated by the AIP model. In the highest collisionality case, π_i approximates δp_i well except for the upstream source region and the vicinity of the sheath entrance. In addition, δp_i itself is small compared to p_i due to high collisionality. Thus, a good agreement between the B2 code and the AIP model is obtained as shown in Fig. 3. In the lowest collisionality case, on the other hand, a clear deviation of π_i from δp_i is seen in the upstream region of a diverging magnetic field in addition to those seen in the highest collisionality case, too. When focusing on this re-

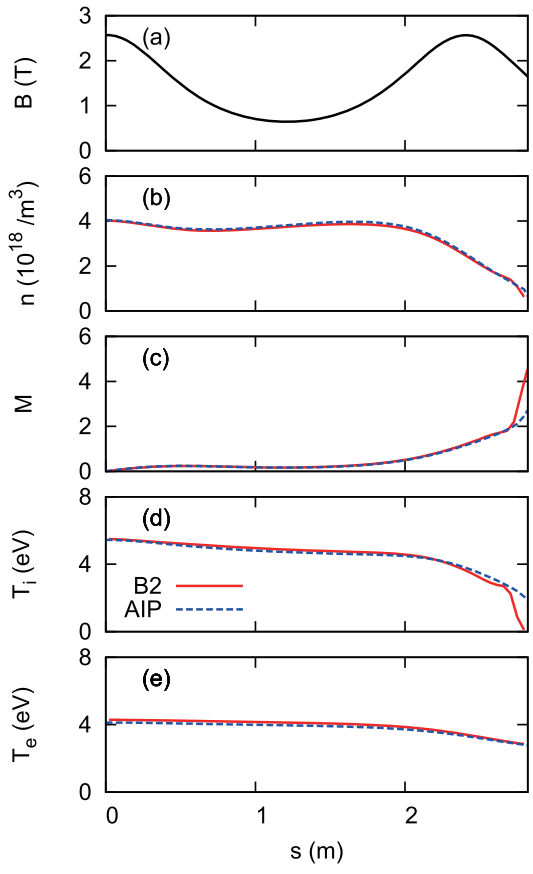

Fig. 3 Profiles of plasma parameters for the highest collisionality case in Fig. 2 (i.e. $L/\lambda_{mfp} \approx 30$) of the B2 code (solid lines) and the AIP model (broken lines); (a) B, (b) n, (c) M, (d) T_i and (e) T_e.

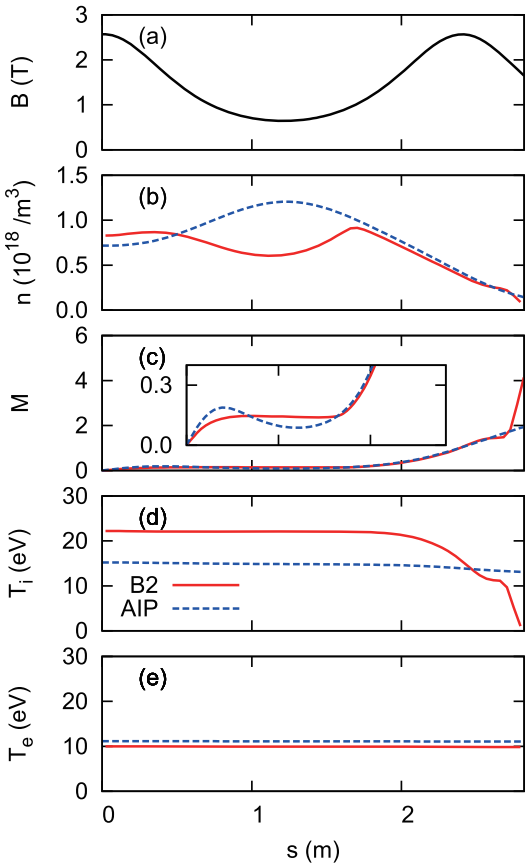

Fig. 4 Profiles of plasma parameters for the lowest collisionality case in Fig. 2 (i.e. $L/\lambda_{\rm mfp} \approx 0.3$) of the B2 code (solid lines) and the AIP model (broken lines); (a) B, (b) n, (c) M with an enlarged view, (d) $T_{\rm i}$ and (e) $T_{\rm e}$.

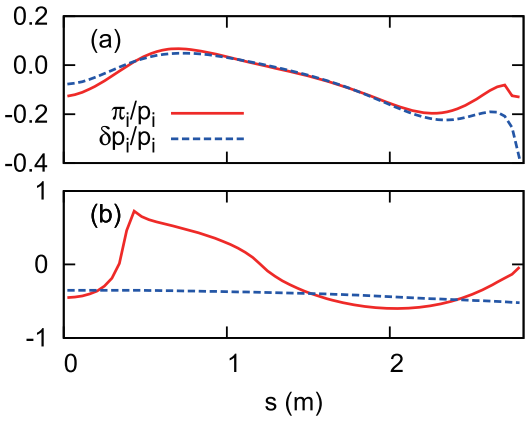

Fig. 5 Profiles of $\pi_{\rm i}$ (solid lines) and $\delta p_{\rm i}$ (broken lines) each of which is normalized by $p_{\rm i}$ estimated by the AIP model for (a) the highest and (b) the lowest collisionality cases.

gion, Eq. (2) can be reduced by assuming the steady state and neglecting the dynamic pressure and $p_{\rm e}$ leading to a rough result of $n \propto B^{\tau}$ in which $\tau \equiv (T_{\rm i,\parallel} - T_{\rm i,\perp})/T_{\rm i,\parallel}$. Because $\delta p_{\rm i}$ and corresponding τ are negative according to Fig. 5 (b), n is negatively correlated with B in the AIP model as shown in Fig. 4 (b). On the other hand, because $\pi_{\rm i}$ is positive in this region according to Fig. 5 (b), τ might also become effectively positive in the B2 code leading to n positively correlated with B as shown in Fig. 4 (b). This invalidity of the viscous-flux approximation probably comes from effects of neglected source terms, the gradient of $\delta p_{\rm i}$ and conductive heat fluxes when it is derived.

4. Summary

A widely-used two-dimensional plasma fluid code B2 which is based on the Braginskii's plasma fluid model has been benchmarked with a one-dimensional plasma fluid model incorporating the anisotropic ion pressures, $p_{\rm i,\parallel}$ and $p_{\rm i,\perp}$ (AIP model) [12, 13] on simple mirror configurations. We obtained nine cases of different plasma collisionalities. In the highest collisionality case, profiles of plasma parameters of the B2 code agree well with those of the AIP model except for the vicinity of the sheath entrance. In the lowest collisionality case, on the other hand, profiles of plasma parameters of the B2 code deviate from those of the AIP model. In addition, supersonic plasma flows downstream from the mirror throat are observed. The validity of the viscous-flux approximation $\pi_{\rm i}$ is also investigated by direct comparisons with the anisotropic part of the ion pressure $\delta p_{\rm i}$ indicating the invalidity of $\pi_{\rm i}$ is considered to be responsible to deviations of profiles.

Acknowledgements

Authors are grateful to Dr. T. Takizuka of Osaka University and Dr. Y. Ogawa of University of Tokyo for a fruitful discussion. This work is partly supported by the IEA Technology Collaboration Programme on the Development and Research on Plasma Wall Interaction Facilities for Fusion Reactors (PWI TCP).

[1] R. Schneider *et al.*, Contrib. Plasma Phys. **46**, 3 (2006).
[2] H. Kawashima *et al.*, Plasma Fusion Res. **1**, 031 (2006).
[3] K. Shimizu *et al.*, Nucl. Fusion **49**, 065028 (2009).
[4] T.D. Rognlien *et al.*, J. Nucl. Mater. **196-198**, 347 (1992).
[5] A.V. Chankin *et al.*, J. Nucl. Mater. **390-391**, 319 (2009).
[6] M. Wischmeier *et al.*, J. Nucl. Mater. **415**, S523 (2011).
[7] M. Groth *et al.*, J. Nucl. Mater. **415**, S530 (2011).
[8] K. Hoshino *et al.*, J. Plasma Fusion Res. Ser. **9**, 592 (2010).
[9] S. Yamoto *et al.*, J. Nucl. Mater. **463**, 615 (2015).
[10] W. Fundamenski, Plasma Phys. Control. Fusion **47**, R163 (2005).
[11] S.I. Braginskii, *Reviews of Plasma Physics*, vol.**1** (Consultants Bureau, New York, 1965) p.205.
[12] S. Togo *et al.*, 16th International Workshop on Plasma Edge Theory in Fusion Devices (2017) O-05.
[13] S. Togo *et al.*, *accepted in* Contrib. Plasma Phys. (2018).
[14] B.J. Braams, NET report no.68 (EUR-FU/XII-80/87/68) (1987).
[15] C. Salmagne and D. Reiter *et al.*, 21st International Conference on Plasma Surface Interactions (2014) O-36.
[16] S. Togo *et al.*, Contrib. Plasma Phys. **56**, 729 (2016).
[17] E. Zawaideh *et al.*, Phys. Fluids **29**, 463 (1986).
[18] S. Togo *et al.*, J. Nucl. Mater. **463**, 502 (2015).
[19] S. Togo *et al.*, J. Comput. Phys. **310**, 109 (2016).